Multiiron Polyoxoanions. Syntheses, Characterization, X-ray Crystal Structures, and Catalysis of H_2O_2-Based Hydrocarbon Oxidations by $[Fe^{III}_4(H_2O)_2(P_2W_{15}O_{56})_2]^{12-}$

Xuan Zhang,[†] Qin Chen,[†] Dean C. Duncan,[†] Charles F. Campana,[‡] and Craig L. Hill*,[†]

Department of Chemistry, Emory University, Atlanta, Georgia 30322

Received June 4, 1997[⊗]

The reaction of $[P_2W_{15}O_{56}]^{12-}$ and aqueous Fe^{3+} forms two ferric polytungstophosphate derivatives that have been isolated, purified, and characterized by X-ray crystallography and several physical methods. At pH ∼3 and $[Na^+] = 2$ M, needles of $Na_{12}[Fe^{III}_4(H_2O)_2(P_2W_{15}O_{56})_2]\cdot 58H_2O$, Na-**1**, form, in which the conventional ion packing arrangement in solid heteropoly acids is observed: each polyanion, $[Fe^{III}_4(H_2O)_2(P_2W_{15}O_{56})_2]^{12-}$ (**1**), is well separated by the cations (Na^+). At pH ∼1 and $[Na^+] = 1$ M, however, elongated prisms of $H_3Na_9[Fe^{III}_4(H_2O)_2(P_2W_{15}O_{56})_2]\cdot 62H_2O$, (Na-**1**)$_n$, form. (Na-**1**)$_n$ is a novel one-dimensional inorganic polymer composed of **1** linked via ion pairing with strongly associated hydrated sodium cations. Both Na-**1** and (Na-**1**)$_n$ display identical characteristics in H_2O solution. Seven lines of evidence are consistent with the Fe^{III}_4 oxidation state in **1**: (1) the synthesis itself (only Fe^{3+} used); (2) bond-length-based valence sum calculations based on the two X-ray structures; (3) the electrochemical behavior; (4) the charge requirements and elemental analyses; (5) no reaction between **1** and Ce^{4+}; (6) the lack of a Jahn−Teller distortion; and (7) the infrared spectrum relative to those of the literature $[M_4(H_2O)_2(P_2W_{15}O_{56})_2]^{16-}$ sandwich compounds, where M = a divalent first-row transition metal ion in all cases. The tetra-*n*-butylammonium salt of **1**, TBA-**1**, exhibits catalytic activity for oxidation of alkenes by H_2O_2. The catalytic effect is substantial. For example, in the reaction of cyclohexene + H_2O_2, rate(with TBA-**1**)/rate(without TBA-**1**) (−d[cyclohexene]/d*t*) is ∼25. Alkene oxidation is characterized predominantly by allylic attack on aliphatic substrates and oxidative cleavage of stilbenes. The polyanion, **1**, is quite stable under catalytic conditions (no decomposition of **1** was detected by ^{31}P NMR after a solution of **1**, alkene, and 0.25 M H_2O_2 was incubated for 48 h).

Introduction

The oxidation or oxygenation of hydrocarbons and other substrates catalyzed by Fe centers in biological and synthetic systems continues to be of considerable fundamental and practical interest.[1−5] Over the last decade, spectroscopic and structural characterization of the Fe_2 active sites in methane monooxygenase (MMO) and ribonucleotide diphosphate reductase (RDPR) have given rise to informative investigations of the actual catalytic mechanism of action of these enzymes.[2,5,6] Simultaneously, a number of synthetic Fe complexes that activate O_2 and/or peroxides and catalyze hydrocarbon oxidation have been reported.[7−9] The mechanistic and synthetic value of these systems has varied significantly, as has the rationale for their development. The impetus for investigation of these complexes has ranged from primarily preparative (useful methods to activate the oxidants and functionalize hydrocarbons and other organic substrates), such as the Gif systems,[10] to primarily elucidating and biomimetic (probes of enzymic mechanism).[7,8]

The most selective homogeneous metal-catalyzed oxidations such as the Halcon process,[11] the Sharpless asymmetric epoxidation,[12,13] and dihydroxylation[14] reactions use oxidants less desirable than H_2O_2 (more expensive and less environmentally benign). One class of homogeneous metal complexes, the

[†] Emory University.
[‡] Siemens Analytical X-ray Systems, Inc.
[⊗] Abstract published in *Advance ACS Abstracts,* August 1, 1997.

(1) Que, L., Jr.; Ho, R. Y. N. *Chem. Rev.* **1996**, *96*, 2607−2624.
(2) Wallar, B. J.; Lipscomb, J. D. *Chem. Rev.* **1996**, *96*, 2625−2657.
(3) Holm, R. H.; Kennepohl, P.; Solomon, E. I. *Chem. Rev.* **1996**, *96*, 2239−2314.
(4) Kurtz, J.; Donald, M. *Chem. Rev.* **1990**, *90*, 585−606.
(5) Rosenzweig, A. C.; Lippard, S. J. *Acc. Chem. Res.* **1994**, *27*, 229−236.
(6) Wilkinson, B.; Zhu, M.; Priestley, N. D.; Nguyen, H.-H. T.; Morimoto, H.; Williams, P. G.; Chan, S. I.; Floss, H. G. *J. Am. Chem. Soc.* **1996**, *118*, 921−922.
(7) Representative earlier studies of non-heme Fe complexes to model the active site in enzymes such as MMO: (a) Vincent, J. B.; Huffman, J. C.; Christou, G.; Li, Q.; Nanny, M. A.; Hendrickson, D. N.; Fong, R. H.; Fish, R. H. *J. Am. Chem. Soc.* **1988**, *110*, 6898−6900. (b) Nam, W.; Valentine, J. S. *New J. Chem.* **1989**, *13*, 677−682. (c) Leising, R. A.; Norman, R. E.; Que, L., Jr. *Inorg. Chem.* **1990**, *21*, 2553−2555. (d) Sheu, C.; Sobkowiak, A.; Jeon, S.; Sawyer, D. T. *J. Am. Chem. Soc.* **1990**, *112*, 8212−8214. (e) Leising, R. A.; Zang, Y.; Que, L., Jr. *J. Am. Chem. Soc.* **1991**, *113*, 8555−8557. (f) Fish, R. H.; Konings, M. S.; Oberhausen, K. J.; Fong, R. H.; Yu, W. M.; Christou, G.; Vincent, J. B.; Coggin, D. K.; Buchanan, R. M. *Inorg. Chem.* **1991**, *30*, 3002−3006. (g) Nam, W.; Ho, R.; Valentine, J. S. *J. Am. Chem. Soc.* **1991**, *113*, 7052−7054. (h) Stassinopoulos, A.; Schulte, G.; Papaefthymiou, G. C.; Caradonna, J. P. *J. Am. Chem. Soc.* **1991**, *113*, 8686−8697. (i) Kang, C.; Redman, C.; Cepak, V.; Sawyer, D. T. *Bioorg. Med. Chem.* **1993**, *1*, 125−140. (j) Ménage, S.; Vincent, J.-M.; Lambeaux, C.; Chottard, G.; Grand, A.; Fontecave, M. *Inorg. Chem.* **1993**, *32*, 4766−4773.
(8) Kim, J.; Harrison, R. G.; Kim, C.; Que, L., Jr. *J. Am. Chem. Soc.* **1996**, *118*, 4373−4379.
(9) Nguyen, C.; Guajardo, R. J.; Mascharak, P. K. *Inorg. Chem.* **1996**, *35*, 6273−6281.
(10) (a) Barton, D. H. R.; Dollar, D. *Acc. Chem. Res.* **1992**, *25*, 504−512. (b) Barton, D. H. R.; Bévière, S. D.; Chavasiri, W.; Csuhai, E.; Doller, D.; Liu, W.-G. *J. Am. Chem. Soc.* **1992**, *114*, 2147−2156. (c) Balavoine, G.; Barton, D. H. R.; Geletti, Y. V.; Hill, D. R. In *Activation of Dioxygen and Homogeneous Catalytic Oxidation*; Barton, D. H. R., Martell, A. E., Sawyer, D. T., Eds.; Plenum Press: New York, 1993; pp 225−242. (d) Singh, B.; Long, J. R.; Papaefthymiou, G. C.; Stavropoulos, P. *J. Am. Chem. Soc.* **1996**, *118*, 2147−2156 and references cited therein.
(11) Parshall, G. W.; Ittel, S. D. *Homogeneous Catalysis. The Applications and Chemistry of Catalysis by Soluble Transition Metal Complexes*, 2nd ed.; Wiley-Interscience: New York, 1992.
(12) Woodward, S. S.; Finn, M. G.; Sharpless, K. B. *J. Am. Chem. Soc.* **1991**, *113*, 106−113.
(13) Finn, M. G.; Sharpless, K. B. *J. Am. Chem. Soc.* **1991**, *113*, 113−126.
(14) Norrby, P. O.; Kolb, H. C.; Sharpless, K. B. *J. Am. Chem. Soc.* **1994**, *116*, 8470−8478.

S0020-1669(97)00690-3 CCC: $14.00

polyperoxotungstates, in particular $\{PO_4[W(O)(O_2)_2]_4\}^{3-}$,[15-23] has exhibited sufficient promise (very high selectivity, reasonable rates, and catalytic properties) for H_2O_2-based epoxidations and other organic oxidations that some processes were commercialized on small scales. Unfortunately, the requirement of chlorinated solvents and the irreversible inactivation of the catalysts after modest numbers of turnovers have conspired thus far to marginalize the viability of these systems.

Early transition metal−oxygen anion clusters or polyoxometalates (POMs for convenience)[24] and their d-electron-transition-metal-substituted polyoxometalate (TMSP) relatives are of interest in catalysis for two general reasons: First, the POM units can function as multidentate totally inorganic and oxidatively resistant ligands for redox-active ions.[25-30] Second, the fundamental properties of POMs that impact homogeneous catalysis and several other applications, including elemental composition, solubility, redox potential(s), charge density, size, and shape, can be systematically altered to a considerable degree. The first generation of TMSPs used as catalysts for the oxidation of organic materials, including the oxygenation of hydrocarbons, were Keggin derivatives.[26] Later TMSPs of other structural classes were used,[28,29] and this literature has been recently reviewed.[30] Sandwich-type TMSPs in which four d-electron transition metal ions link two trivacant Keggin and Wells−Dawson fragments appear quite promising as a potential class of oxygenation catalysts because both the heteroatoms in the trivacant POM units and the four central metal ions can be varied considerably. Since the first Keggin-derived complexes of formula $[(TM^{II})_4(H_2O)_2(PW_9O_{34})_2]^{10-}$ were reported by Weakley, Tourné, and co-workers[31,32] and the first Wells−Dawson-derived complexes of formula $[(TM^{II})_4(H_2O)_2(P_2W_{15}O_{56})_2]^{16-}$ were reported by Finke and Droege,[33] the number of sandwich-type TMSPs reported in the literature has increased manyfold.[34-43]

Recently our group reported H_2O_2-based epoxidation catalyzed by Fe sandwich POMs that exhibited reasonable rates, selectivities, and stabilities.[44] More recently, Neumann and coworkers reported that another sandwich-type TMSP complex, $[WZnMn^{II}_2(ZnW_9O_{34})_2]^{12-}$, initially prepared by Tourné,[34] was a superior catalyst for H_2O_2-based epoxidation.[45] More recently still, the isostructural Ru and Rh analogs prepared by the Neumann laboratory, were also shown to be excellent catalysts for this reaction.[40,46]

This paper addresses the speciation of Fe^{3+}(aq) and the trivacant heteropolytungstate α-$[P_2W_{15}O_{56}]^{12-}$, derived from the well-known Wells−Dawson POM α-$[P_2W_{18}O_{62}]^{6-}$. The principal product, a sandwich complex of formula $[Fe^{III}_4(H_2O)_2(P_2W_{15}O_{56})_2]^{12-}$, **1**, is a trivalent (TM^{III}_4) analog of the literature Finke-type complexes of formula $[(TM^{II})_4(H_2O)_2(P_2W_{15}O_{56})_2]^{16-}$ (best characterized for TM = Co, Cu, and Zn).[33,43,47,48] The polyanion **1**, has been characterized by X-ray crystallography in two different forms, a conventional monomeric form and a novel polymeric form. Additional examination of this polyanion by FTIR, UV−visible, ^{31}P NMR, EPR, and Mössbauer spectroscopies and cyclic voltammetry clearly defines its electronic and other selected properties. The ability of **1** to catalyze oxidation of alkenes by H_2O_2 in acetonitrile and its stability in the presence of H_2O_2 are assessed.

Experimental Section

General Methods and Materials.

$Na_{12}[P_2W_{15}O_{56}]\cdot 18H_2O$ was prepared by the method of Finke et al.[47] Acetonitrile and other solvents (Burdick and Jackson) were used as received. The alkenes were reagent grade from Fluka or Aldrich, and purities were checked by gas chromatography (GC). C, H, N analyses were performed by Atlantic Microlab Inc., Norcross, GA. All other elemental analyses were performed by E+R Microanalytical Laboratory Inc., Corona, NY. The alkene products were identified by GC (Hewlett-

(15) Venturello, C.; D'Aloiso, R.; Bart, J. C.; Ricci, M. *J. Mol. Catal.* **1985**, *32*, 107−110.
(16) Amato, G.; Arcoria, A.; Ballistreri, F. P.; Tomaselli, G. A.; Bortolini, O.; Conte, V.; Difuria, F.; Modena, G.; Valle, G. *J. Mol. Catal.* **1986**, *37*, 165−175.
(17) *Hydrogen Peroxide Oxidation Catalyzed by Heteropoly Acids Combined with Cetylpyridium Chloride*; Ishii, Y., Ogawa, M., Eds.; MYU: Tokyo, 1990; Vol. 3, pp 121−145.
(18) Aubry, C.; Chottard, G.; Platzer, N.; Brégeault, J.-M.; Thouvenot, R.; Chauveau, F.; Huet, C.; Ledon, H. *Inorg. Chem.* **1991**, *30*, 4409−4415.
(19) Dengel, A. C.; Griffith, W. P.; Parkin, B. C. *J. Chem. Soc., Dalton Trans.* **1993**, 2683−2688.
(20) Ballistreri, F. P.; Bazzo, A.; Tomaselli, G. A.; Toscano, R. M. *J. Org. Chem.* **1992**, *57*, 7074−7077.
(21) Salles, L.; Aubry, C.; Thouvenot, R.; Robert, F.; Dorémieux-Morin, C.; Chottard, G.; Ledon, H.; Jeannin, Y.; Brégeault, J.-M. *Inorg. Chem.* **1994**, *33*, 871−878.
(22) Duncan, D. C.; Chambers, R. C.; Hecht, E.; Hill, C. L. *J. Am. Chem. Soc.* **1995**, *117*, 681−691.
(23) Griffith, W. P.; Parkin, B. C.; White, A. J. P.; Williams, D. J. *J. Chem. Soc., Chem. Commun.* **1995**, 2183−2184.
(24) Pope, M. T.; Müller, A. *Angew. Chem., Int. Ed. Engl.* **1991**, *30*, 34−48.
(25) Katsoulis, D. E.; Pope, M. T. *J. Am. Chem. Soc.* **1984**, *106*, 2737−2738.
(26) Hill, C. L.; Brown, R. B., Jr. *J. Am. Chem. Soc.* **1986**, *108*, 536−538.
(27) Hill, C. L. In *Activation and Functionalization of Alkanes*; Hill, C. L., Ed.; Wiley: New York, 1989; pp 243−279.
(28) Mansuy, D.; Bartoli, J.-F.; Battioni, P.; Lyon, D. K.; Finke, R. G. *J. Am. Chem. Soc.* **1991**, *113*, 7222−7226.
(29) Representative papers addressing catalysis by TMSP complexes: (a) Faraj, M.; Hill, C. L. *J. Chem. Soc., Chem. Commun.* **1987**, 1487−1489. (b) Schwegler, M.; Floor, M.; van Bekkum, H. *Tetrahedron Lett.* **1988**, *29*, 823−826. (c) Faraj, M.; Lin, C.-H.; Hill, C. L. *New J. Chem.* **1988**, *12*, 745−749. (d) Neumann, R.; Abu-Gnim, C. *J. Chem. Soc., Chem. Commun.* **1989**, 1324−1325. (e) Katsoulis, D. E.; Pope, M. T. *J. Chem. Soc., Dalton Trans.* **1989**, 1483−1488. (f) Fedotov, M. A.; Il'inich, O. M.; Kuznetsova, L. I.; Semin, G. L.; Vetchinova, Y. S.; Zamaraev, K. I. *Catal. Lett.* **1990**, *6*, 417−422. (g) Neumann, R.; Abu-Grim, C. J. *J. Am. Chem. Soc.* **1990**, *112*, 6025−6031. (h) Mansuy, D.; Bartoli, J.-F.; Battioni, P.; Lyon, D. K.; Finke, R. G. *J. Am. Chem. Soc.* **1991**, *113*, 7222−7226. (i) Lyons, J. E.; Ellis, P. E., Jr.; Durante, V. A. In *Stud. Surf. Sci. Catal.*; R. A. Grasselli and A. W. Sleight, Eds.; Elsevier Scientific: Amsterdam, 1991; Vol. 67; pp 99−116. (j) Rong, C.; Pope, M. T. *J. Am. Chem. Soc.* **1992**, *114*, 2932−2938. (k) Steckhan, E.; Kandzia, C. *Synlett* **1992**, 139−140; (l) Khenkin, A. M.; Hill, C. L. *J. Am. Chem. Soc.* **1993**, *115*, 8178−8186.
(30) Hill, C. L.; Prosser-McCartha, C. M. *Coord. Chem. Rev* **1995**, *143*, 407−455.
(31) Weakley, T. J. R.; Evans, H. T., Jr.; Showell, J. S.; Tourné, G. F.; Tourné, C. M. *J. Chem. Soc., Chem. Commun.* **1973**, 139−140.
(32) Evans, H. T.; Tourné, C. M.; Tourné, G. F.; Weakley, T. J. R. *J. Chem. Soc., Dalton Trans.* **1986**, 2699−2705.
(33) Finke, R. G.; Droege, M. W. *Inorg. Chem.* **1983**, *22*, 1006−1008.
(34) Tourné, C. M.; Tourné, G. F.; Zonnevijlle, F. *J. Chem. Soc., Dalton Trans.* **1991**, 143−155.
(35) Wasfi, S. H.; Rheingold, A. L.; Kokoszka, G. F.; Goldstein, A. S. *Inorg. Chem.* **1987**, *26*, 2934−2939.
(36) Wasfi, S. H. *Synth. React. Inorg. Met.-Org. Chem.* **1989**, *19*, 1059−1068.
(37) Knoth, W. H.; Domaille, P. J.; Farlee, R. D. *Organometallics* **1985**, *4*, 62−68.
(38) Knoth, W. H.; Domaille, P. J.; Harlow, R. L. *Inorg. Chem.* **1986**, *25*, 1577−1584.
(39) Neumann, R.; Khenkin, A. M.; Dahan, M. *Angew. Chem., Int. Ed. Engl.* **1995**, *34*, 1587−1589.
(40) Neumann, R.; Khenkin, A. M. *Inorg. Chem.* **1995**, *34*, 5753−5760.
(41) Gómez-García, C. J.; Coronado, E.; Gómez-Romero, P.; Casañ-Pastor, N. *Inorg. Chem.* **1993**, *32*, 3378−3381.
(42) Gómez-García, C. J.; Coronado, E.; Ouahab, L. *Angew. Chem., Int. Ed. Engl.* **1992**, *31*, 649−651.
(43) Gómez-García, C. J.; Borrás-Almenar, J. J.; Coronado, E.; Ouahab, L. *Inorg. Chem.* **1994**, *33*, 4016−4022.
(44) Khenkin, A. M.; Hill, C. L. *Mendeleev Commun.* **1993**, 140−141.
(45) Neumann, R.; Gara, M. *J. Am. Chem. Soc.* **1995**, *117*, 5066−5074.
(46) Neumann, R.; Khenkin, A. M. *J. Mol. Catal.* **1996**, *114*, 169−180.
(47) Finke, R. G.; Droege, M. W.; Domaille, P. J. *Inorg. Chem.* **1987**, *26*, 3886−3896.
(48) Weakley, T. J. R.; Finke, R. G. *Inorg. Chem.* **1990**, *29*, 1235−1241.

Packard 5890 gas chromatograph fitted with a flame ionization detector, a 25-m × 0.2-mm 5% phenyl methyl silicone capillary column, nitrogen carrier gas, and a Hewlett-Packard 3390A integrator) and by gas chromatography−mass spectrometry (GC/MS; Hewlett-Packard 5890 Series II gas chromatograph coupled with a Hewlett-Packard 5971A mass selective detector). Infrared spectra (2% sample in KBr or acetonitrile solutions) were recorded on a Nicolet 510M FTIR instrument. The electronic absorption spectra were taken on a Shimadzu UV-2101 PC UV−visible spectrophotometer. ^{31}P broad-band NMR spectra were measured on a General Electric GN-500 spectrometer utilizing 85% H_3PO_4 with D_2O in a capillary insert as a reference. Average magnetic susceptibilities were measured on a Johnson Matthey Model MSB-1 magnetic susceptibility balance as neat powders at 24 °C; the balance was calibrated using $Hg[Co(SCN)_4]$ as a standard.[49] Pascal's constants were used to obtain the final diamagnetic corrections. EPR spectra were recorded at X-band frequency with a Bruker ER 200D spectrometer equipped with a helium cryostat at 8, 50, 200, and 297 K. EPR samples were prepared at 1 mM concentrations as optically transparent glasses in the ternary solvent system $CH_3CN-CH_2Cl_2-C_6H_5CH_3$ (1:2:4 and 1:4:6 by volume for TBA-**1**). Cyclic voltammetry was performed using standard PAR instrumentation in a three-electrode arrangement: glassy carbon disk working electrode (Bioanalytical Systems), a Pt wire auxiliary electrode, and a reference electrode. The reference electrode was saturated calomel with 1 M NaCl as the supporting electrolyte in aqueous solution. ^{57}Fe Mössbauer measurements were made using a weak-field Mössbauer spectrometer equipped with a Janis 8DT cryostat.

Synthesis of $H_3Na_9[Fe^{III}_4(H_2O)_2(P_2W_{15}O_{56})_2]\cdot 62H_2O$, (Na-1)$_n$, and $Na_{12}[Fe^{III}_4(H_2O)_2(P_2W_{15}O_{56})_2]\cdot 58H_2O$, Na-1. These complexes were prepared by a modification of the procedure used for the literature tetranuclear divalent Wells−Dawson-derived sandwich complexes of formula $[(TM)_4(H_2O)_2(P_2W_{15}O_{56})_2]^{16-}$ (TM = one of several first-row divalent cations).[47] The polymeric complex, (Na-**1**)$_n$, was prepared as follows. To a solution of 0.82 g (3 mmol) of $FeCl_3\cdot 6H_2O$ in 40 mL of H_2O was added slowly with vigorous stirring 6.0 g (1.5 mmol) of α-$Na_{12}[P_2W_{15}O_{56}]$. The solution was heated at 80 °C until the volume was reduced to ∼22 mL. NaCl (1.5 g, 26 mmol) was added. The solution was filtered hot and the supernatant left unstirred in a beaker open to the air. After 1−2 days, orange columnar crystals formed (1.8 g, 30% yield).

The complex with the monomeric motif, Na-**1**, was prepared by a slightly different procedure as follows. To a solution of 0.82 g (3 mmol) of $FeCl_3\cdot 6H_2O$ in 30 mL of 2 M NaCl solution was added slowly with vigorous stirring 6.0 g (1.5 mmol) of α-$Na_{12}[P_2W_{15}O_{56}]$. The solution was heated to 80 °C for 5 min and filtered hot. The filtrate was left in the air. After several days, a yellow crystalline solid formed (1.8 g, 30% yield). X-ray-quality crystals of Na-**1** were obtained by recrystallizing 1 g of the yellow solid from 5 mL of 2 M NaCl solution. The needle-shaped crystals of Na-**1** were dichroic: yellow along the short axis and brown along the long axis.

The spectroscopic properties of Na-**1** and (Na-**1**)$_n$ were indistinguishable, and as a consequence, only one set of spectroscopic data is given unless stated otherwise. Electronic absorption spectral data (400−800 nm, in H_2O) [λ, nm (ϵ, M^{-1} cm^{-1})]: 480.8 sh (131). IR (2% KBr pellet, 1300−400 cm^{-1}): 1091 (s), 1017 (w), 951 (s, sh), 917 (m), 826 (s), 757 (s), 695 (s), 630 (m, sh), 526 (w). ^{31}P NMR (9 mM solution in H_2O; D_2O in capillary insert): one resonance for the distal P atoms at −11.1 ppm, $\Delta\nu_{1/2}$ = 70 Hz. Magnetic susceptibility: μ_{eff} = 10.3 μ_B/mol at 297 K. EPR and ^{57}Fe Mössbauer: no signals. Anal. Calcd for $H_{131}Cl_{0.5}Fe_4Na_{9.5}O_{176}P_4W_{30}$, (Na-**1**·0.5NaCl)$_n$: Cl, 0.20; Fe, 2.48; Na, 2.41; P, 1.37; W, 61.16. Found: Cl, 0.18; Fe, 2.24; Na, 2.73; P, 1.20; W, 61.06. Calcd for $H_{120}ClFe_4Na_{13}O_{172}P_4W_{30}$, Na-**1**·NaCl: Cl, 0.39; Fe, 2.46; Na, 3.30; P, 1.37; W, 60.81. Found: Cl, 0.48; Fe, 2.35; Na, 3.30; P, 1.24; W, 60.93. The NaCl of crystallization cannot be avoided for either complex, as both must be crystallized from aqueous NaCl solution. They can also be crystallized from aqueous NaBr solution. Only amorphous material is produced from salt-free H_2O, however.

Synthesis of $[(C_4H_9)_4N]_{11.5}H_{0.5}Fe^{III}_4(H_2O)_2P_4W_{30}O_{112}$ (TBA-1). (Na-**1**)$_n$ (1.6 g, 0.2 mmol) was dissolved in 40 mL of H_2O. Tetra-*n*-butylammonium (TBA) chloride (3.0 g, 10 mmol) was added with stirring. To the cloudy yellow solution was added 200 mL of CH_2Cl_2. The mixture was shaken in a separatory funnel to obtain an almost colorless upper aqueous phase and a clear yellow lower organic phase. The organic layer was collected in a round-bottom flask and concentrated to a thick oil using a rotary evaporator. After being washed with 10 mL of water, the oil solidified, and the solid was dried under water aspirator vacuum. The yellow solid was redissolved in a minimum amount of CH_3CN, and an excess quantity (ca. 100 mL) of diethyl ether was added to afford a bright yellow powder (1.4 g, 80% yield). The compound was recrystallized by dissolving 0.08 g of the crude product in 6 mL of a 5:1 v/v mixture of CH_3CH_2OH and CH_3CN, followed by ether diffusion at −20 °C. The spectroscopic properties establish that **1** had not changed during the conversion of (Na-**1**)$_n$ to TBA-**1**. Electronic absorption spectral data (400−800 nm, in H_2O) [λ, nm (ϵ, M^{-1} cm^{-1})]: 483.4 sh (149). IR (2% KBr pellet, 1300−400 cm^{-1}): 1093 (s), 1018 (w), 955 (s), 916 (s), 894 (m, sh), 829 (s), 801 (s, sh), 758 (s), 681 (m), 625 (m), 528 (w). ^{31}P NMR (9 mM solution in CH_3CN; D_2O in capillary insert): one resonance for the distal P atoms at −9.7 ppm, $\Delta\nu_{1/2}$ = 80 Hz. Anal. Calcd for $C_{184}H_{418.5}Fe_4N_{11.5}O_{114}P_4W_{30}$: C, 21.09; H, 4.03; Fe, 2.13; N, 1.54; P, 1.18; W, 52.63. Found: C, 20.97; H, 3.93; Fe, 1.69; N, 1.54; P, 1.02; W, 52.90.

X-ray Crystallography. $H_3Na_9[Fe^{III}_4(H_2O)_2(P_2W_{15}O_{56})_2]\cdot 62H_2O$, (Na-1)$_n$. A light yellow prismatic crystal (0.44 × 0.20 × 0.16 mm) coated with Paratone-N was immediately placed in a stream of liquid-nitrogen vapor (temperature set at −100 °C) and centered on a standard Siemens SMART CCD Area Detector System equipped with a normal-focus molybdenum-target X-ray tube. A total of 1321 frames of data were collected using a narrow-frame method with scan widths of 0.3° in ω and an exposure time of 30 s/frame ($2\theta_{max}$ = 56.69°). Frames were integrated with the Siemens SAINT program to yield a total of 22 132 reflections, of which 16 090 were independent (R_{int} = 4.99%, R_{sig} = 4.34%) and 15 810 were above $4\sigma(F)$. The crystal was face-indexed for absorption corrections. The corrected data were used for subsequent solution and refinement. Crystal data, details of the intensity measurements, and data processing parameters are summarized in Table 1. The structure was solved by direct methods[50] and refined by full-matrix-least-squares-on-F^2 techniques (15 810 reflections with $F^2 > 2\sigma(F_o^2)$),[51] using anisotropic temperature factors for all atoms. At final convergence, R = 5.09% and GOF = 1.10 for 1007 parameters.

$Na_{12}[Fe^{III}_4(H_2O)_2(P_2W_{15}O_{56})_2]\cdot 58H_2O$, Na-1. Crystals of Na-**1** lose transparency instantly upon exposure to air. A suitable X-ray-quality crystal (0.40 × 0.38 × 0.18 mm) taken from the mother liquor was immediately mounted in inert oil on a glass fiber and centered at −100 °C on a Siemens P4 four-circle diffractometer equipped with graphite-monochromated Mo Kα radiation (λ = 0.710 73 Å). A total of 10 140 reflections ($2\theta_{max}$ = 45°) were collected using the ω-scan mode with variable speeds (5−30°/min). The reflection statistics indicated the centrosymmetric nature of the crystal lattice. The data were corrected for absorption using the empirical ψ-scan method, and the corrected data were used for subsequent solution and refinement. Crystal data, details of the intensity measurements, and data processing parameters are summarized in Table 1. Direct methods were used to solve the structure. The initial model containing the skeleton of the asymmetric unit (15 tungsten atoms, two iron atoms, and two phosphorus atoms) was expanded with subsequent refinement based on the full-matrix-least-squares-on-F^2 techniques (9597 reflections with $F^2 > 2\sigma(F_o^2)$). Anisotropic temperature factors were applied to all atoms (W, Fe, P, and O) in the polyanion, $[Fe^{III}_4(H_2O)_2(P_2W_{15}O_{56})_2]^{12-}$, **1**, and isotropic temperature factors were applied to the cationic sodium atoms and water molecules of crystallization. Disorder in some of the sodium cations and water molecules due to thermal motion was observed. Partial occupancies were used for several water molecules with higher temperature factors during the final stage of refinement. At final convergence, R = 0.0997 and GOF = 1.037 for 842 parameters.

Procedure for **Catalytic Oxidations (Table 3).** In a typical reaction, a mixture of TBA-**1** (0.004 mmol in 1 mL of CH_3CN) and alkene (0.9

(49) Figgis; Nyholm. *J. Chem. Soc.*, **1958**, 4190.

(50) *SHELXTL PC*; Siemens Analytical X-ray Instruments, Inc.: Madison, WI, 1990.

(51) Sheldrick, G. M. *SHELX 93*: *Program for structure refinement*; University of Goettingen: Goettingen, Germany, 1993.

Table 1. Crystallographic Data for (Na-**1**)$_n$ and Na-**1**

	(Na-**1**)$_n$	Na-**1**
empirical formula	$H_{131}Fe_4Na_9O_{176}W_{30}$	$H_{120}Fe_4Na_{12}O_{172}P_4W_{30}$
fw	9017.74	9007.59
cryst color	light yellow	light yellow
cryst shape	elongated prisms	needles
cryst system	triclinic	triclinic
space group	$P\bar{1}$ (No. 2)	$P\bar{1}$ (No. 2)
a, Å	12.5836(1)	12.558(3)
b, Å	15.9516(2)	16.128(3)
c, Å	19.4233(3)	19.010(5)
α, deg	87.048(1)	87.34(2)
β, deg	83.268(1)	80.65(2)
γ, deg	75.322(1)	75.00(2)
V, Å^3	3744.61(8)	3670(2)
Z	1	1
ρ_{calcd}, Mg m^{-3}	3.999	4.076
μ, mm^{-1}	23.512	23.99
diffractometer	Siemens SMART CCD Area Detector System	Siemens P4
temp, K	173	173
radiation λ, Å	0.710 73	0.710 73
θ range, deg	1.09−28.34	1.09−22.5
scan speed, deg/min in ω		5−30
scan width (ω), deg	0.3	
exposure time, s/frame	30	
abs cor	face index	empirical ψ scans
no. of reflcns	16 090	10 140
no. of restraints	234	342
no. of params	1007	842
R_1 [$I > 2\sigma(I)$][a]	0.0509	0.0997
wR_2[b]	0.1198	0.2630
GOF	1.101	1.037

[a] $R_1 = \sum||F_o| - |F_c||\sum|F_o|$. [b] $wR_2 = \{[\sum w(F_o^2 - F_c^2)^2]/\sum w(F_o^2)^2]\}^{1/2}$.

mmol) was thoroughly degassed and purged with argon at 25 °C. The mixture was stirred at 500 rpm, and reaction was initiated by the addition of 25 μL of 30% aqueous H_2O_2. The organic products were analyzed and quantified with GC or GC/MS using decane or trimethylacetonitrile as the internal standard.

To assess the stability of **1** under catalytic conditions, a representative reaction solution (cyclohexene as substrate), with the concentrations of **1**, alkene, and H_2O_2 given above, was stirred under Ar for 48 h. The solvent was then removed in vacuo. The resulting solid was redissolved in ~0.3 mL of CH_3CN and examined by ^{31}P NMR (D_2O in a capillary insert was used for locking).

Results and Discussion

Synthesis of the Tetrairon Sandwich Polyoxoanions, (Na-1)$_n$ and Na-1. The complexes (Na-**1**)$_n$ and Na-**1** were readily prepared in ~30% isolated yields and in high purity. The tetra-*n*-butylammonium salt, TBA-**1**, was prepared by metathesis of either Na-**1** or (Na-**1**)$_n$ in H_2O. Figure 1 shows the ^{31}P NMR spectra of both Na-**1** in aqueous solution and TBA-**1** in CH_3CN solution. The best preparation of Na-**1** is similar in some respects to that used for the literature sandwich polytungstophosphate complexes, $[M_4(H_2O)_2(P_2W_{15}O_{56})_2]^{16-}$, all of which involve divalent first-row transition metal ions (best characterized for M = Co(II), Mn(II), Cu(II), and Zn(II)).[47] Three factors are important in the synthesis: the use of (i) isomerically pure α-$Na_{12}[P_2W_{15}O_{56}]$, (ii) stoichiometric quantities of Fe^{3+} relative to the polytungstophosphates, and (iii) soluble Fe^{3+} only (in our hands, (Na-**1**)$_n$ and Na-**1** could not be made from either $Fe^{2+} + O_2$ or $Fe^{2+} + H_2O_2$). In contrast to the neutral pH observed during the synthesis of divalent sandwich compounds, the solution pH during the synthesis of tetranuclear Fe^{III} complexes remains very low (pH ~1) throughout addition of α-$Na_{12}[P_2W_{15}O_{56}]$. α-$Na_{12}[P_2W_{15}O_{56}]$, added as a solid, dissolves readily in the $FeCl_3$ solution even at room temperature, and no insoluble intermediates are observed during the addition. In contrast, the synthesis of all the literature $[M^{II}_4(H_2O)_2(P_2W_{15}O_{56})_2]^{16-}$ complexes requires heating for reaction completion. See the Experimental Section for complete details.

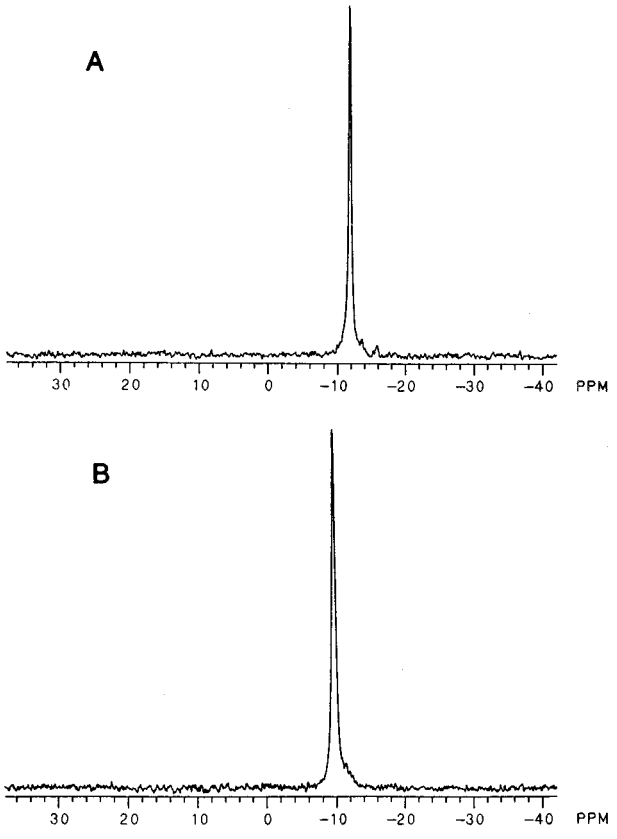

Figure 1. ^{31}P NMR spectra of **1**: (A) (Na-**1**)$_n$ (9 mM solution in H_2O); (B) TBA-**1** (9 mM solution in CH_3CN). D_2O in a capillary insert was used for locking in both cases.

Crystal Growth and X-ray Structures of (Na-1)$_n$ and Na-1. The pH and Na concentration affect not only the morphology

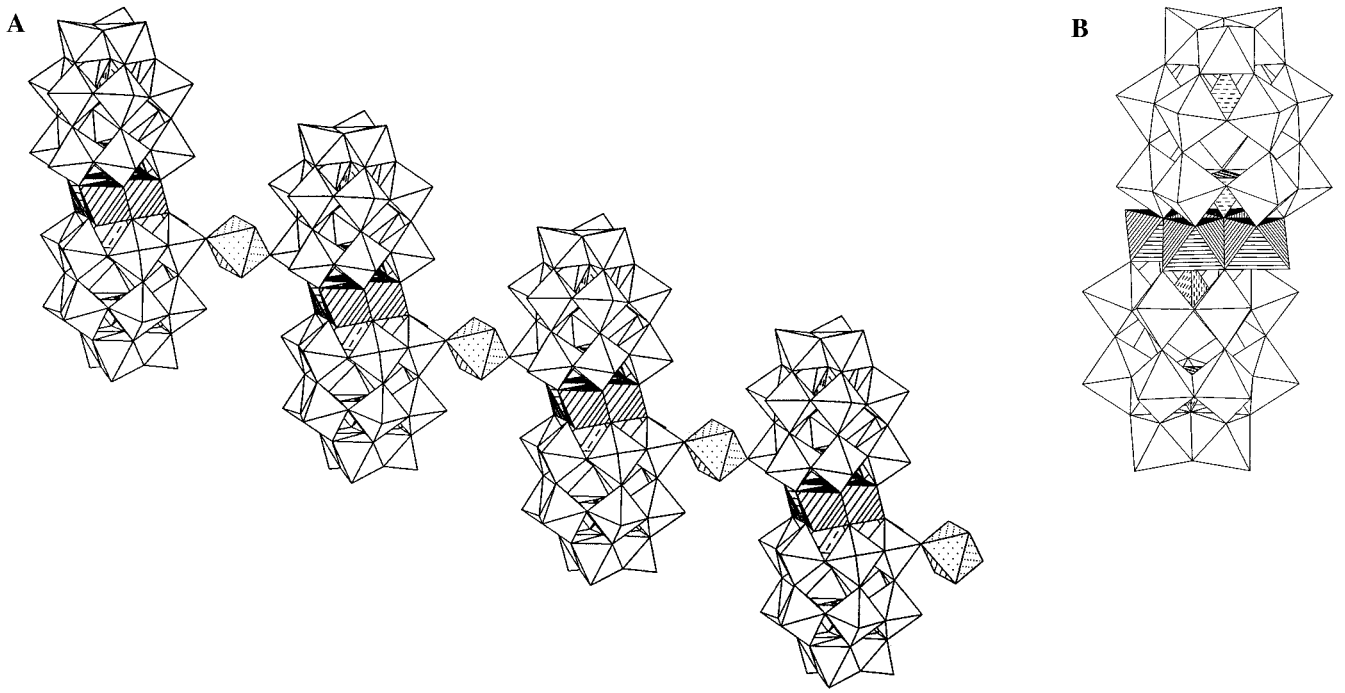

Figure 2. (A) Polyhedral representation of the polymeric array in (Na-**1**)$_n$. (B) Polyhedral representation of **1** in Na-**1**. The W octahedra are blank, the Fe octahedra are parallel lines, the internal P tetrahedra are dashed parallel lines, and the bridging sodium octahedra are dotted.

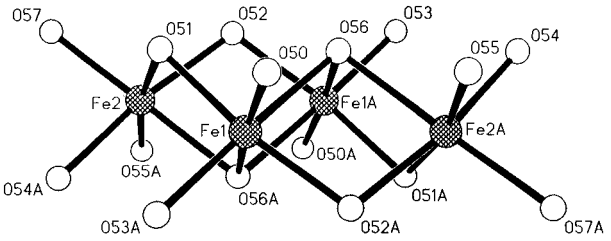

Figure 3. Structure of the central tetrameric unit in **1**, $Fe_4O_{14}(H_2O)_2$.

(external form) of the crystals but, more fundamentally, their composition and structure. At high acidity (pH ∼1) and low Na concentration (∼1 M), crystals of (Na-**1**)$_n$ form exclusively. At lower acidity (pH ∼3) and higher Na concentration (∼2 M), crystals of Na-**1** form. For (Na-**1**)$_n$, the crystals are column-shaped (elongated prisms) with color ranging from orange to brown depending on the size of the crystal, and single crystals are readily obtained. For Na-**1**, the crystals are usually stacked needles. The crystals are dichroic, yellow along the short axis and brown along the long axis. Single crystals are difficult to obtain; extensive cutting is necessary.

Figures 2−4 and Table 2 summarize the X-ray structural data for both (Na-**1**)$_n$ and Na-**1**. Figure 2 illustrates the two structures in polyhedral notation, Figure 3 gives a ball-and-stick representation of the central $Fe_4O_{14}(H_2O)_2$ unit, Figure 4 shows an ORTEP drawing of the asymmetric unit in (Na-**1**)$_n$, and Table 2 provides key distances and angles for both (Na-**1**)$_n$ and Na-**1**. The polyanion, **1**, is nearly identical in both structures, and the key distances for purposes of the subsequent structure description are taken from (Na-**1**)$_n$, as these crystals were of higher quality than the crystals of Na-**1**.

The polyanion **1** consists of an oxo−aqua tetranuclear iron core, $[Fe^{III}_4O_{14}(H_2O)_2]$, sandwiched by two trivacant α-Wells−Dawson structural moieties, α-$[P_2W_{15}O_{56}]$. The polyanion, **1**, has C_{2h} symmetry and approximate axial (P1···P2 direction) and equatorial dimensions of 21.88 and 10.64 Å, respectively.

One sodium ion (Na1) in (Na-**1**)$_n$, situated at the crystallographic inversion center and ligated by four water molecules (O1s, O2s, O1sa, and O2sa), bridges two different molecules

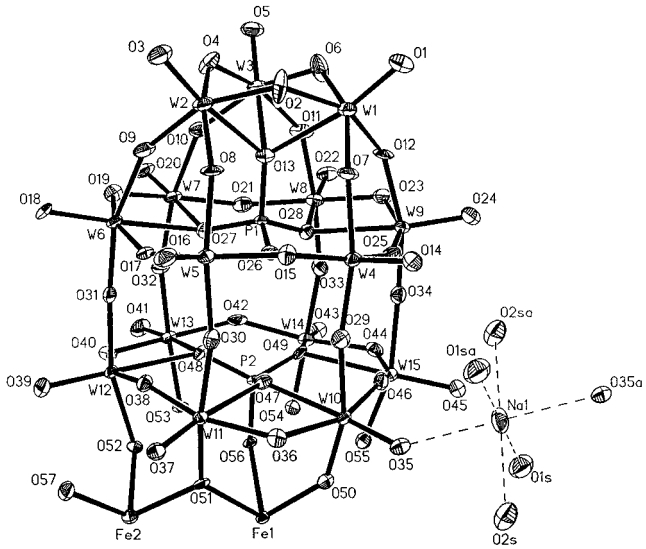

Figure 4. ORTEP drawing of the asymmetric unit of (Na-**1**)$_n$, showing the complete coordination around Na1 at the crystallographic inversion center.

of **1** by dative bonding to an oxygen on each (O35 and O35a) to form a highly unusual one-dimensional array illustrated in polyhedral notation in Figure 2A. In most crystallographically characterized heteropolyanion complexes, the polyanions are well separated by both solvent molecules (often H_2O) and countercations and do not form polymeric species.[52,53] The partial disorder in the lattice makes it problematical to distinguish some sodium cations and water molecules from each other; this is commonly observed in heteropolyanion X-ray structures.[54] The location of the linking sodium cation (Na1) at the

(52) Gimenezsaiz, C.; Galanmascaros, J. R.; Triki, S.; Coronado, E.; Ouahab, L. *Inorg. Chem.* **1995**, *34*, 524−526.

(53) One other sandwich polyanion appears to be linked in a polymeric motif, the $[Cu_4(H_2O)_2(P_2W_{15}O_{56})_2]$ complex of Weakley and Finke. See paragraph 5, p 1238, in: Weakley, T. J. R.; Finke, R. G. *Inorg. Chem.* **1990**, *29*, 1235−1241.

(54) See footnote 13 in: Weakley, T. J. R.; Finke, R. G. *Inorg. Chem.* **1990**, *29*, 1235−1241.

Table 2. Selected Bond Lengths (Å) and Bond Angles (deg) for $(Na\text{-}\mathbf{1})_n$ and Na-**1**[a]

	$(Na\text{-}\mathbf{1})_n$	Na-**1**		$(Na\text{-}\mathbf{1})_n$	Na-**1**
W−O_t	1.715(10)	1.701(22)	O_t−W−O_b (cap)	102.2(5)	104.4(11)
W−O_b	1.909(10)	1.896(20)	O_t−W−O_b (belt)	99.7(5)	99.5(10)
W−O_c	2.368(9)	2.363(20)	O_t−W−O_d (cap)	169.9(4)	168.2(10)
W−O_d	2.370(10)	2.373(20)	O_t−W−O_d (belt)	172.6(4)	172.0(10)
P−O_c	1.531(9)	1.513(20)	O_d−P−O_c	107.0(5)	107.6(12)
P−O_d	1.592(10)	1.610(20)	O_d′−P−O_c	107.2(5)	107.3(11)
P−$O_{d'}$	1.607(9)	1.620(20)	Fe1···Fe2···Fe1A	63.6(5)	64.4(10)
Fe1···Fe2	3.194(10)	3.173(20)	Fe2···Fe1···Fe2A	116.4(5)	115.6(10)
Fe1···Fe1A	3.364(10)	3.381(20)	W10−O35−Na1	134.5(5)	
Fe1···Fe2A	3.190(10)	3.173(20)	O35−Na1−O1s	93.7(4)	
Fe2···Fe2A	5.425(9)	5.374(20)	O35−Na1−O2s	82.1(4)	
Fe1−O50	1.900(9)	1.910(20)	O1s−Na1−O2s	95.4(4)	
Fe1−O51	2.021(9)	1.990(20)			
Fe1−O52A	2.017(9)	1.990(20)			
Fe1−O53A	1.905(9)	1.890(20)			
Fe1−O56	2.219(9)	2.190(20)			
Fe1−O56A	2.184(9)	2.170(20)			
Fe2−O51	2.035(9)	2.060(20)			
Fe2−O52	2.022(9)	2.040(20)			
Fe2−O54A	1.958(9)	1.990(20)			
Fe2−O55A	1.965(10)	1.930(20)			
Fe2−O56A	2.185(9)	2.170(20)			
Fe2−O57	2.043(10)	2.050(20)			
W10−O35	1.707(9)	1.720(20)			
Na1−O35	2.334(10)				
Na1−O1s	2.381(12)				
Na1−O2s	2.490(20)				

[a] O_t = terminal oxygen; O_b = doubly bridging oxygen; O_c = triply bridging oxygen; O_d = quadruply bridging oxygen; $O_{d'}$ = quadruply bridging oxygen that bonds to the Fe atoms.

crystallographic special position in $(Na\text{-}\mathbf{1})_n$ is unambiguous on the basis of four criteria: (i) its peak height in the difference Fourier map, (ii) its coordination geometry, (iii) the refinement results, and (iv) the consistency in two different structure determinations of $(Na\text{-}\mathbf{1})_n$. The lengths of the Na1−O35 and W10−O35 bonds that define the linkages between the polyanions are 2.334(10) and 1.707(9) Å, respectively.

The X-ray structure of the conventional (nonpolymeric) complex, Na-**1**, is shown in Figure 2B. Because the quality of these crystals and the subsequent structure determination, while reasonable, was not as high as that for $(Na\text{-}\mathbf{1})_n$ (see Tables 1 and 2), three complete data sets on Na-**1** crystals from two different samples were collected and solved. As Table 2 indicates, the bond distances and angles of **1** are nearly identical in $(Na\text{-}\mathbf{1})_n$ and Na-**1**.

The structure of the $Fe_4O_{14}(H_2O)_2$ unit, shown in Figure 3, is similar to those of the M_4 units in the divalent heteropolytungstates of formula $[M_4(H_2O)_2(P_2W_{15}O_{56})_2]^{16-}$ (M = Cu(II), Zn(II), Mn(II)).[43,47,48] The central four iron atoms lie in the same plane, and their edge-sharing FeO_6 octahedra resemble a rhombus with sides of 3.194 and 3.190(9) Å, a short and long diagonal of 3.364 and 5.425(9) Å, and angles between Fe atoms of 63.6(4) and 116.4(5)°. Each of the seven vertices on both faces of the rhombus, which are all occupied by oxo groups, is corner-shared with two α-$[P_2W_{15}O_{56}]$ units, leaving the remaining one vertex on each side of the inversion center (located at the midpoint of the Fe2···Fe2A vector) occupied by an aqua group (O57 and O57a) with a bond (Fe2−O57) distance of 2.043(10) Å. The $Fe_4O_{14}(H_2O)_2$ unit in **1**, like the $Mn^{II}_4O_{14}(H_2O)_2$ unit in $[Mn_4(H_2O)_2(P_2W_{15}O_{56})_2]^{16-}$ [43] but unlike the $Cu^{II}_4O_{14}(H_2O)_2$ unit in the analogous copper complex, shows little or no Jahn−Teller distortion consistent with four $S = {}^5/_2$ Fe(III) ions. The Fe−O axial and equatorial distances around the Fe atoms in **1** range from 2.021 to 2.185(9) Å and from 1.900 to 2.219(9) Å, respectively. The Fe atoms in **1**, like the central metal ions in the Zn^{II}_4 and Mn^{II}_4 analogs and unlike those in the Cu^{II}_4 analog, are positioned symmetrically around the P2···P1 vector.

The central Fe atoms, the cap W atoms (W1−W3), and the two sets of belt W atoms (W4−W9 and W10−W15) in **1** form four least-squares planes with a maximum deviation of 0.012 Å. They are parallel to each other with a maximum dihedral angle of 0.6°. In the Zn^{II}_4, Mn^{II}_4, and Cu^{II}_4 analogs, the maximum deviation in any of these four planes is 0.047 Å and the maximum dihedral angle is ∼1°. In comparison, the four least-squares planes in α-$[P_2W_{18}O_{62}]^{6-}$ (two planes each composed of three cap W atoms and two planes each composed of six belt W atoms) have a maximum deviation of 0.041 Å and a maximum dihedral angle of 0.4°.[55] The α-$[P_2W_{15}O_{56}]^{12-}$ unit derived from α-$[P_2W_{18}O_{62}]^{6-}$ in **1** appears to be less distorted upon coordination to the central tetrameric unit, and the displacements of phosphorus atoms from their W belts relative to the $Fe^{III}_4O_{14}(H_2O)_2$ unit are less significant as compared with those in the divalent analogs, $[M^{II}_4(H_2O)_2(P_2W_{15}O_{56})_2]^{16-}$. This derives from the lack of Jahn−Teller distortion and a favorable interplay of charge and radius ratios of all atoms in the cluster. The P2 atom is displaced only 0.133 Å from the M_4O_{16} plane as compared to 0.179, 0.185, and 0.194 Å in the Zn^{II}_4, Mn^{II}_4, and Cu^{II}_4 complexes, and the P1 atoms are displaced 0.136 Å toward the M_4O_{16} unit as compared to 0.222, 0.183, and 0.186 Å in the Zn^{II}_4, Mn^{II}_4, and Cu^{II}_4 complexes. The average Fe···P2 distance in **1** is 3.329(9) Å (Fe1···P2 = 3.338(9) Å, Fe2···P2 = 3.310(9) Å, and Fe1A···P2 = 3.333(9) Å). Also of note is that all the trans-directed bonds along the cluster axial direction, M(Fe)−O−W_{belt}−O−W_{belt}−O_{cap}−W_{cap}, in **1** have less pronounced bond length alterations (average distances: 1.964, 1.854, 1.977, 1.968, 1.884(9) Å) than those in the divalent derivatives (average distances: 2.12, 1.78, 2.05, 1.79, 1.99, and 1.86 Å).

Physical Properties of $(Na\text{-}\mathbf{1})_n$ and Na-1. Electronic Structure of 1. These two forms are distinguishable only by X-ray crystallography. The IR spectra and magnetic susceptibility of the two solids as well as the ^{31}P NMR and UV−visible absorption spectra of solutions of the two complexes are identical. The $\sim\nu_3$ vibrational mode of the PO_4 unit in the IR spectrum of **1** is very similar in energy to that in the spectrum of the parent polytungstophosphate, α-$[P_2W_{18}O_{62}]^{6-}$. The absence of splitting in this PO_4 peak indicates that this unit is less perturbed from pure T_d symmetry in **1** than in the corresponding divalent sandwich complexes that exhibit splittings of ∼30 cm^{-1}.[56] This is consistent with the X-ray crystallographic structural features discussed above. The yellow-orange complexes display no sharp maxima for the Fe-centered d−d bands in the visible region because the intense oxygen-to-metal-charge-transfer (OMCT) bands in the UV region characteristic of all d^0 polyoxometalates tail into the blue and dominate the entire electronic absorption spectrum. The complete absence of W-based d−d bands and intervalence-charge-transfer (IVCT) absorption bands, indicative of one or more W(V) ions in the polyanion,[57] rules out the presence of such sites in **1**. The ambient-temperature magnetic moments of $(Na\text{-}\mathbf{1})_n$ and Na-**1** (10.3 μ_B) imply some degree of antiferromagnetic coupling. The effective spin-only moment for a ferromagnetically coupled $S = 10$ system is 21.0 μ_B. The paramagnetic ground electronic state renders only one signal clearly observable in the ^{31}P NMR spectrum, that for the P atoms

(55) D'Amour, H. *Acta Crystallogr., Sect. B: Struct. Sci.* **1976**, *32*, 729.
(56) Rocchiccioli-Deltcheff, C.; Thouvenot, R. *J. Chem. Res., Synop.* **1977**, *2*, 46−47.
(57) Pope, M. T. *Heteropoly and Isopoly Oxometalates*; Springer-Verlag: Berlin, 1983.

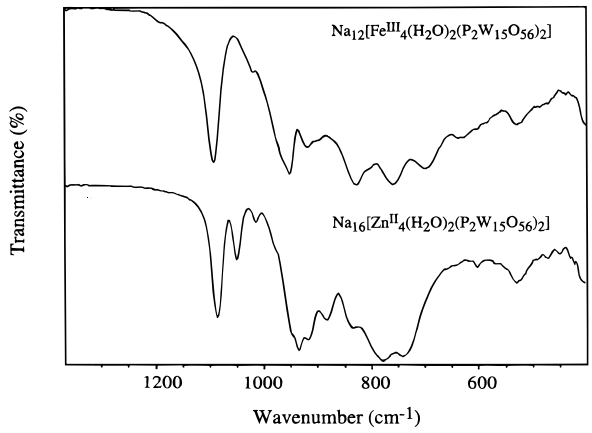

Figure 5. Infrared spectra of **1** (top) and the nearly isostructural tetranuclear divalent species, $[Zn_4(H_2O)_2(P_2W_{15}O_{56})_2]^{16-}$ (bottom).

distal to the Fe_4 unit (−11.1 ppm, $\Delta\nu_{1/2}$ = 70 Hz). The complexes are EPR silent.

The cyclic voltammogram of **1** exhibits three principal unresolved reduction peaks at 0.14, 0.05, and −0.13 V (vs NaCl-saturated SCE) and three corresponding oxidation peaks at 0, 0.13, and 0.22 V corresponding to the Fe(III/II) redox processes. The first polyanion reduction peak is at −1.01 V. The rest potential of a solution of **1** is 0.3 V, which is anodic of the Fe(III/II) potential. A substantial cathodic stripping peak at −0.55 V is a reproducible feature in the cyclic voltammetric behavior of **1** on glassy carbon. This peak is more sensitive to the history of the glassy carbon working electrode surface than the other peaks and likely derives from potential-dependent partly reversible electrode surface modification processes (the stripping peak disappears when the lower limit of the potential is set at −0.8 V). The potential-dependent modification of working electrode surfaces by polyoxotungstates has been studied at some length although some structural characteristics of such phases remain elusive.[58−60]

While the measured Fe(III/II) and W(VI/V) potentials in **1** indicate that $Fe^{II}_xFe^{III}_{4-x}$, x = 1−3, species would be stable (intramolecular reduction of W(VI) by Fe(II) is highly unfavorable), seven lines of evidence are consistent with the Fe^{III}_4 oxidation state in **1**: First, **1** is prepared with Fe^{3+} as the only Fe source, and reduction of Fe^{3+} to Fe^{2+} in the synthetic medium is very unlikely. Second, bond-length-based valence sum calculations[61] from both X-ray structures yield average oxidation states for Fe of 2.84 ± 0.07 in (Na-**1**)$_n$ and 2.88 ± 0.15 in Na-**1**. Third, the rest potential in the cyclic voltammograms of **1** indicates this molecule is fully oxidized. Fourth, the charge requirements for the anions and cations based on the X-ray structure and the elemental analyses are most consistent with Fe^{III}_4. Fifth, addition of 1 equiv of Ce(IV) to an aqueous solution of **1** results in no reduction of Ce. Sixth, the lack of significant Jahn−Teller distortion is more consistent with S = $^5/_2$ Fe(III) centers than with Fe(II) centers. Seventh (indirect evidence), the infrared spectrum of **1** is distinct from that of the nearly isostructural divalent literature complexes, $[M_4(H_2O)_2(P_2W_{15}O_{56})_2]^{16-}$, where M = Zn(II) and Cu(II). Figure 5 is exemplary: the IR spectra of **1** and $[Zn_4(H_2O)_2(P_2W_{15}O_{56})_2]^{16-}$ are compared. Because ^{57}Fe Mössbauer spectra would further address the oxidation and spin state assignments of the Fe atoms in **1**, repeated attempts were made to obtain spectra. In all cases, unfortunately, excessive scattering reduced the signals to negligible intensity.

Table 3. Organic Products from Oxidation of Representative Alkenes with H_2O_2 Catalyzed by **1**[a]

Substrate	Products Selectivity [initial rate, mM/hr][b]		
	 11% [0.133]	 40% [0.469]	 48% [0.566]
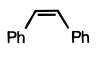	 25% [0.125]	 c	PhCHO 74% [0.374]
	 88% [0.570]	 c	 11% [0.077]

[a] Reaction conditions: 25 μL of 30% aqueous H_2O_2 was injected into 1 mL of an CH_3CN solution of **1** (4 mM) and alkene substrate (0.9 M) under Ar to initiate the reaction. Aliquots (1.5 μL) of reaction mixtures were removed at calibrated time intervals and analyzed by GC. [b] Selectivity = moles of indicated product/moles of all organic products derived from substrate [initial rate = slope of the indicated product vs time plot when the conversion is less than 1%]. [c] No detectable reaction (detection limit <0.2%).

Alkene Oxidation by H_2O_2 Catalyzed by TBA-1. The TBA salt of **1** is very soluble in polar organic solvents and catalyzes the facile oxidation of alkenes by H_2O_2 at 25 °C. The catalytic effect varies with the particular alkene, and a representative value of rate(with TBA-**1**)/rate(without TBA-**1**), for cyclohexene + H_2O_2, is ∼25.

Table 3 reports the oxidation of representative alkenes by H_2O_2 catalyzed by TBA-**1** in CH_3CN solution and the distribution of alkene-derived oxidation products. CH_3CN rather than a chlorocarbon was used as the solvent. While chlorocarbons (usually $CHCl_3$, $ClCH_2CH_2Cl$, or CH_2Cl_2) are the most common solvents in recent studies of homogeneous metal-catalyzed H_2O_2-based oxidations because they are often more effective for such reactions, they are sufficiently toxic that their use counteracts the potential benefit of using the environmentally friendly oxidant H_2O_2. In addition, an effort was undertaken to report the alkene-derived products in this study not merely as yields after a particular reaction time (one data point per reaction), which is the usual case in such studies, but also as initial rates (several data points per reaction) because such data are more informative regarding mechanism. The lower the conversion, the fewer product-distribution-altering subsequent processes are potentially operable. The data in Table 3 clearly indicate that oxidation of alkenes by H_2O_2 catalyzed by **1** exhibits low selectivity with allylic attack on aliphatic alkenes and oxidative cleavage of a representative aromatic substrate, *trans*-stilbene, predominating over epoxidation. These selectivities are consistent with oxy radicals and/or high-valent oxo−iron intermediates as the substrate-attacking species in the mechanism. A single mechanism involving a metal-bound and electrophilically activated peroxo species transferring oxygen to alkene, the predominant mechanism in the well-established Sharpless asymmetric epoxidation and Halcon processes, is very unlikely.

The polyanion, **1**, is quite stable under catalytic conditions. No decomposition of **1** was detected by ^{31}P NMR after a solution of **1**, alkene, and 0.25 M H_2O_2 was incubated for 48 h.

(58) Keita, B.; Nadjo, L. *Mater. Chem. Phys.* **1989**, *22*, 77−103.
(59) Keita, B.; Nadjo, L. *J. Electroanal. Chem. Interfacial Electrochem.* **1993**, *354*, 295−304.
(60) Nadjo, L.; Keita, B. *J. Phys.* **1994**, *4*, 329−336.
(61) O'Keeffe, M.; Navrotsky, A. *Structure and Bonding in Crystals*; Academic Press: New York, 1981.

Acknowledgment. This research was supported by the National Science Foundation (Grant CHE-9022317). We also acknowledge the Office of Naval Research (Molecular Design Institute; Grant N00014-95-1-1116) for partial support of this work. We thank the Molecular Structure Corp. and Dr. Rene J. Lachicotte of Rochester University for their assistance with the X-ray crystal structure determinations and Professor Vincent Huynh of the Emory University Department of Physics for the attempted acquisition of Mössbauer spectra.

Supporting Information Available: Tables giving details of the structure determinations, atomic coordinates and equivalent isotropic displacement coefficients, bond lengths and bond angles, and anisotropic displacement parameters for (Na-**1**)$_n$ and Na-**1** (24 pages). Ordering information is given on any current masthead page.

IC970690G